NMR Studies on the Self-Association of Uridine and Uridine Analogues

Anita Dunger, Hans-Heinrich Limbach, and Klaus Weisz*

Abstract: Association constants for the dimerization of acylated uridine and two analogues, 4-thiouridine and 6-oxadihydrouridine, have been determined in chloroform solution. At 293 K, self-association constants K were found to decrease in the order uridine > 6-oxadihydrouridine > 4-thiouridine. Low-temperature 1D and 2D NMR measurements in a deuterated freon mixture allowed the unambiguous assignment of the different dimeric species formed. For homodimers of uridine, the 2- and 4-carbonyl groups act as H-bond acceptors with equal frequency, whereas for the 6-oxa analogue the 2-carbonyl is strongly favored over the 4-carbonyl group. No hydrogen bonding of the 4-S atom is observed in the 4-thio analogue. In agreement with the more negative atomic charge on the O4 oxygen predicted from ab initio calculations, ^{1}H chemical shifts of the H-bonded proton in uridine dimers indicate a stronger hydrogen bond in the 4- as compared to the 2-position.

Keywords: hydrogen bonds · isotopic labeling · nucleic acids · nucleosides

Introduction

Association of nucleobases by specific hydrogen bonds is a major determinant of nucleic acid structure. Thus, the double helix of DNA is based on the specific recognition of guanosine (G) by cytidine (C) and of adenosine (A) by thymidine (T) to form Watson–Crick base pairs. However, because of the multiple proton donor and acceptor sites, configurations other than Watson–Crick pairings are conceivable for the association of nucleobases. Such nonstandard base pairs, far from being mere curiosities, frequently occur in DNA and RNA structures. Examples include reverse Watson–Crick base pairs in parallel-stranded DNA,[1] Hoogsteen hydrogen bonding in triple helices[2] or U–U base pairing in RNA.[3a–c] Besides their central role in determining the three-dimensional structure of nucleic acids, the properties of hydrogen-bond donor and acceptor sites in nucleobases are crucial for the rapidly developing technologies based on molecular recognition. These include the design of synthetic host compounds[4] or of DNA-specific ligands like antisense and antigene agents.[5]

Because of this importance, numerous theoretical[6a–d] and some experimental studies[7a–f] on the association of nucleobases have been performed in the past. While a considerable amount of thermodynamic data for base–base interactions in aprotic solvents has been collected, the detailed structure of the associates in solution is still a matter of debate. On the basis of IR[8] as well as NMR spectroscopic studies[9a–d] at ambient temperature, preferred association modes for homo- and heterodimers of nucleobases have been proposed, yet no reliable evaluation of the various dimer populations has been possible so far.

As a first step we have performed NMR measurements on a uridine derivative at very low temperatures in a freon mixture.[10] This enabled us for the first time to observe individual nucleoside base pairs in solution by NMR methods. To further explore the preferred hydrogen-bonding scheme of nucleobases and its modulation by chemical modifications, we have studied the association of suitably derivatized ^{15}N-labeled uridine and of two uridine analogues by homo- and heteronuclear NMR spectroscopic techniques at low and ambient temperatures. The uridine analogues are derived from the uracil base by replacing the exocyclic 4-carbonyl oxygen by sulfur and the 6-methine group by an oxygen atom. 4-Thiouracil is formed in post-transcriptional reactions and found as a constituent in tRNA molecules. The synthetic 6-oxa analogue is an isoster of 5,6-dihydrouracil and has been shown to be an apparent competitive antagonist of uracil in bacterial systems.[11] Whereas the first substitution directly alters an H-bond acceptor site of the uracil base, the second analogue is composed of a different heterocyclic ring system with unchanged H-bond donor and acceptor functionalities. The modifications introduced in **2** and **3** are shown to have a marked effect on the association modes of the nucleoside. In addition, ^{15}N NMR data are presented and discussed for their potential use for monitoring hydrogen bonding.

[*] Dr. K. Weisz, Dipl.-Phys. A. Dunger, Prof. Dr. H.-H. Limbach
Institut für Organische Chemie der Freien Universität Berlin
Takustr. 3, D-14195 Berlin (Germany)
Fax: (+ 49) 30-838-5310
E-mail: weisz@chemie.fu-berlin.de

  0947-6539/98/0404-0621 $ 17.50+.25/0

Results and Discussion

Nucleoside self-association: We have studied the self-association of the specifically ^{15}N-labeled nucleosides [3-^{15}N]-2′-deoxyuridine (**1**), [3-^{15}N]-2′-deoxy-4-thiouridine (**2**), and [3-^{15}N]-6-oxadihydrouridine (**3**) (Figure 1a). As shown in Table 1, the pK_a of the nucleoside decreases by about a unit from uridine to the 6-oxa- and the 4-thioketo analogue. However, irrespective of their structural differences, the same possible association modes must be considered for each of the three bases. In contrast to DNA or RNA oligonucleotides, hydrogen bonding and base pairing of the free monomers can be studied without restrictions imposed by steric and electrostatic interactions of the sugar–phosphate backbone. Theoretical and experimental evidence suggests that at least two cyclic hydrogen bonds must form to produce a stable base pair.[13] Accordingly, nucleosides **1**, **2**, and **3** can be arranged in four different configurations depending on the use of the 4- or 2-carbonyl group as proton acceptor for each of the two bases in the homodimer (Figure 1b). Dimers **I** and **II** with an O(S)4–O(S)4 and an O2–O2 pairing have a C_2 axis of symmetry. The two configurations O(S)4–O2 and O2–O(S)4 are of course identical in the case of self-association and are represented by the asymmetric dimer **III**.

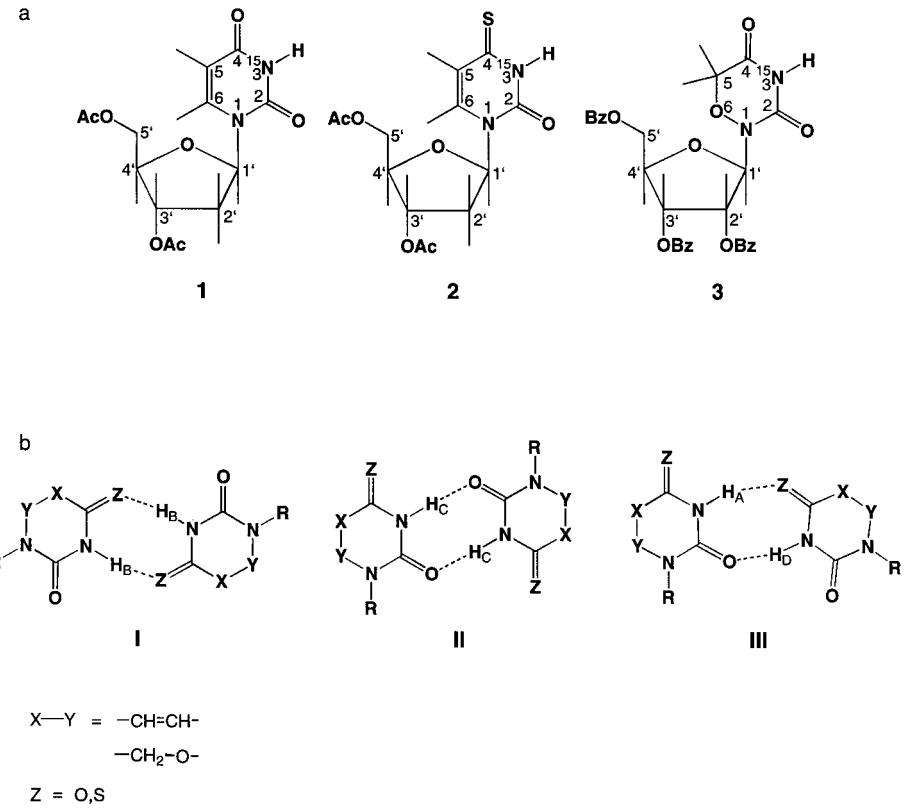

Figure 1. a) Structure of acylated [3-^{15}N]-2′-deoxyuridine (**1**), [3-^{15}N]-2′-deoxy-4-thiouridine (**2**), and [3-^{15}N]-6-oxadihydrouridine (**3**) with atom numbering indicated.[12] b) Possible cyclic dimers formed by self-association of **1**, **2**, and **3**.

In order to determine equilibrium constants for self-association, we measured ^1H chemical shifts for the imino proton of the nucleosides as a function of concentration. For apolar solvents, acylation of the free sugar OH groups is necessary to enhance nucleoside solubility. Isotherms for the three nucleosides in $CDCl_3$ at 20 °C are shown in Figure 2. A nonlinear least-squares fit of the data to a fast monomer–dimer equilibrium yields association constants that are summarized in Table 1. The self-association constants decrease by an overall factor of 4 in the order **1** > **3** > **2**. Available literature values for 1-cyclohexyluracil in chloroform range from $3.2 < K < 6.1\,M^{-1}$,[7d, e, 9a] while for 1-cyclohexyl-4-thiouracil a value of $K = 2.7\,M^{-1}$ was determined using infrared methods.[7d] Although our values are noticeably higher, there is still good agreement with the published data

Table 1. pK_a values, equilibrium constants K and free enthalpies ΔG of self-association for nucleosides **1**, **2**, and **3** at 293 K.

Nucleoside	Solvent	pK_a[a]	K (M^{-1})	ΔG (kJ mol^{-1})
1	$CDCl_3$	9.3[13]	12.7	−6.2
2	$CDCl_3$	8.2[13]	3.1	−2.8
3	$CDCl_3$	8.7[14]	5.3	−4.1
1[a]	H_2O	9.3[13]	0.0[b]	±0.0[b]

[a] Nonacylated derivatives in aqueous solution. [b] From concentration dependent 3-^{15}N chemical shift.

Abstract in German: *Die Assoziationskonstanten für die Dimerisierung von acyliertem Uridin und der beiden Analoga 4-Thiouridin und 6-Oxadihydrouridin in Chloroform wurden ermittelt. Die Gleichgewichtskonstanten für die Selbstassoziation nehmen dabei in der Reihe Uridin > 6-Oxadihydrouridin > 4-Thiouridin bei 293 K ab. 1D- und 2D-NMR-Messungen in einem Gemisch aus deuterierten Freonen bei tiefen Temperaturen ermöglichten eine eindeutige Zuordnung der unterschiedlichen Dimerstrukturen. In den Homodimeren von Uridin fungieren die 2- und die 4-Carbonylgruppe in gleichem Maße als H-Brückenacceptoren, während die 2-Carbonylgruppe in der analogen 6-Oxa-Verbindung ein wesentlich besserer Acceptor ist als die 4-Carbonylfunktion. Für die 4-Thio-Verbindung kann keine Beteiligung des 4-S-Atoms an Wasserstoffbrücken nachgewiesen werden. In Übereinstimmung mit dem durch Ab-initio-Rechnungen erhaltenen Befund, daß die Ladung an O4 etwas negativer ist als die an O2, deuten die ^1H-NMR-Verschiebungen der H-Brücken-gebundenen Protonen in den Uridindimeren auf eine stärkere Wasserstoffbrükkenbindung unter Einbeziehung der 4-Position hin.*

0947-6539/98/0404-0622 $ 17.50+.50/0 *Chem. Eur. J.* **1998**, *4*, No. 4

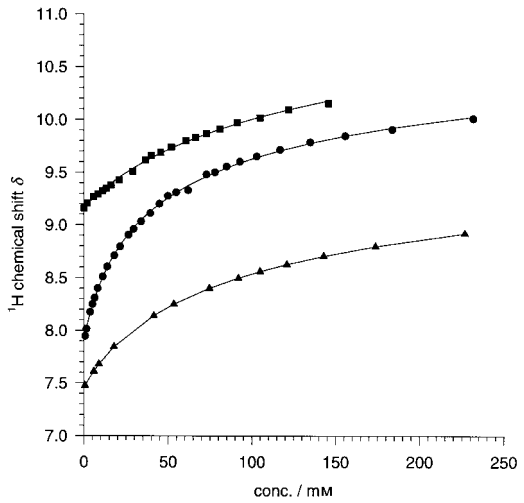

Figure 2. Concentration dependence of the imino proton chemical shift in $CDCl_3$ for **1** (●), **2** (■), and **3** (▲) at 293 K. Lines represent the least-squares fit.

given the different residues and the lower temperature in our studies (293 K vs. 298–303 K). Note also that self-association of nonderivatized uridine in H_2O is negligible, that is, 3-^{15}N chemical shifts were found to be essentially independent in this solvent within the concentration range $416 > c > 13$ mM (data not shown). Clearly, the water molecules effectively compete for the H-bond donor and acceptor sites, thus disrupting any homodimeric species.

Structure of nucleoside dimers: Data obtained from ^{1}H chemical shift measurements at room temperature represent averages over all coexisting dimeric species and do not allow a detailed evaluation of type and relative population of the self-associates present in solution. However, concentration-dependent ^{13}C chemical shifts measured for both the C-2 and C-4 carbonyl carbon of 1-cyclohexyluracil in chloroform indicated that both the 4- and 2-carbonyl act as proton acceptor sites in dimer formation.[9a] Also, the probability that the 4-carbonyl group was used was found to decrease in the 4-thiouracil derivative. In contrast, similar ^{13}C NMR experiments on a uridine derivative in acetonitrile were interpreted to indicate a predominant O4–O4 dimer.[9c] Such a dimer is also observed in the solid state of 1-methyluracil[15] and was considered the major dimeric species based on ^{17}O NMR measurements of uracil in dimethylsulfoxide.[9b] Finally, Kyogoku et al. concluded from IR spectroscopic studies on 1-cyclohexyluracil that one U–U dimer predominates in chloroform solution, although which one could not be determined.[8] However, similar association constants for all three dimers, as calculated for the 5-methyl analogue 1-methylthymine in the gas phase,[6b] could also account for their experimental data.

In order to study the preferred association modes of the nucleosides **1**, **2**, and **3** in more detail we performed NMR measurements at temperatures low enough for any coexisting dimers to be in slow exchange. For this purpose, a deuterated freon mixture $CDClF_2/CDF_3$ was used as solvent, allowing measurements in the liquid state down to 100 K.[16a–c] Besides serving as a nuclear probe for H-bond interactions, the ^{15}N isotope has the advantage in ^{1}H NMR measurements of reducing the linewidth of the attached imino proton upon ^{15}N decoupling.

*[3-^{15}N]-3′,5′-Diacetyl-2′-deoxyuridine (**1**):* ^{1}H NMR spectra showing the imino proton resonances of **1** in freon are plotted as a function of temperature in Figure 3a. Upon cooling, the signal initially shifts downfield as a result of increased formation of hydrogen-bonded dimers. At 133 K the resonance broadens considerably and finally splits into four separate signals at 123 K with chemical shifts of $\delta = 12.36$ (A), 12.24 (B), 11.84 (C), and 11.72 (D). Obviously, these resonances can be attributed to different coexisting dimeric species in slow exchange (Figure 1b).

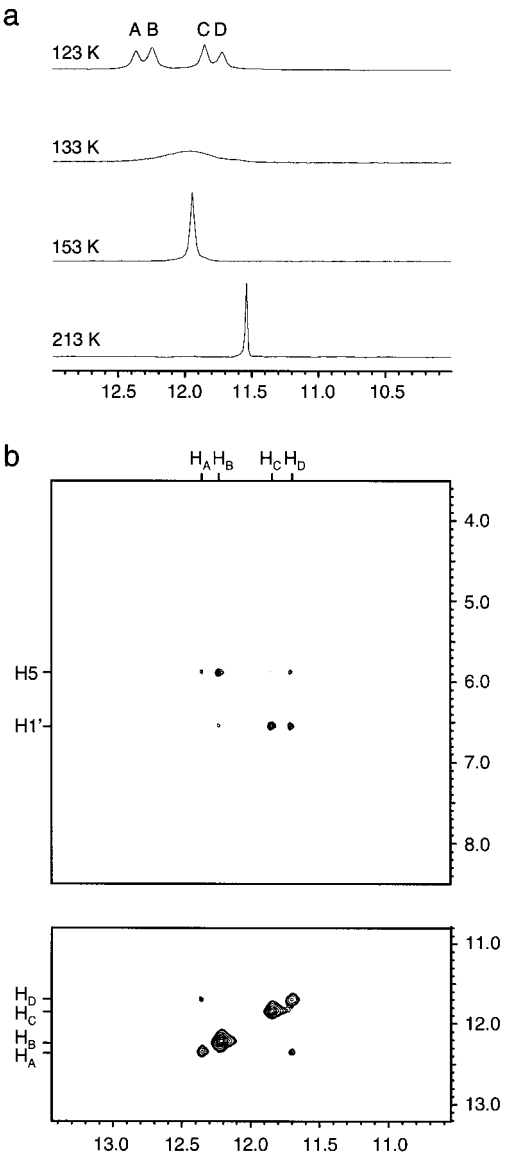

Figure 3. a) Imino proton spectral region of ^{1}H{^{15}N} NMR spectra of **1** in freon as a function of temperature. b) Portion of a ^{1}H{^{15}N} 2D NOE spectrum of **1** in freon showing imino–imino (bottom) and imino–base/sugar proton crosspeaks (top). The spectrum was acquired at 113 K with a 60 ms mixing time.

In order to unambiguously assign the four imino resonances at low temperatures, we performed a homonuclear 2D NOE experiment at 113 K. At this temperature no crosspeaks due to chemical exchange are observed and NOE contacts directly identify protons in close spatial proximity. Regions of the 2D NOE spectrum showing imino proton contacts are plotted in Figure 3b. Prominent crosspeaks connect the two imino resonances H_A and H_D at $\delta = 12.36$ and 11.72, the two downfield-shifted imino signals H_A and H_B with H5 and the two upfield-shifted imino signals H_C and H_D with H1′ protons. In a model for the three cyclic dimers of **1,** short interproton distances involving imino protons can be identified (Figure 4).

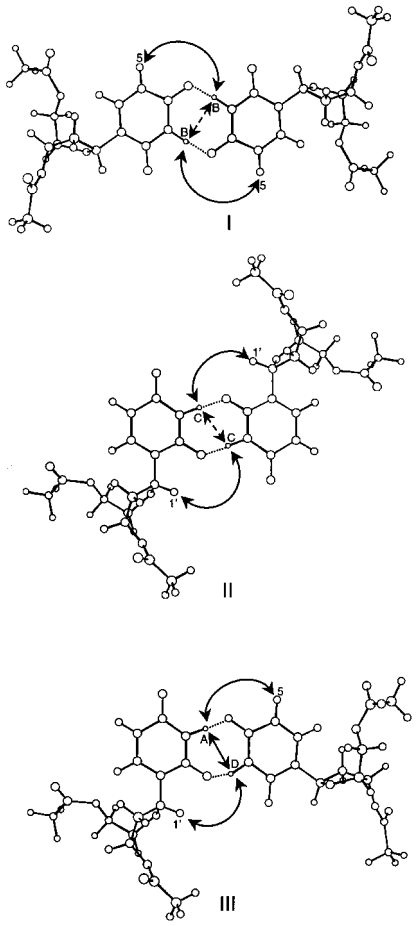

Figure 4. Models of the three cyclic dimers of **1** in their *anti* conformation. Arrows indicate short interproton distances < 4 Å to the imino protons, with dashed arrows connecting two equivalent imino protons that give no observable NOE contact.

Thus, intermolecular NOE connectivities are expected between the two nonequivalent imino protons of the O4 – O2 dimer **III**, as well as between imino protons hydrogen-bonded to the 4-carbonyl group and H5 with distances of about 3.0 and 3.6 Å, respectively. Intermolecular distances between imino protons hydrogen-bonded to the 2-carbonyl group and the anomeric H1′ proton depend on the O4′-C1′-N1-C2 glycosidic torsion angle κ. However, the two main conformations, *syn* and *anti*, are easily distinguished by their different NOE patterns between the base H6 and sugar protons.[17] For **1,** intramolecular NOE contacts observed between H6 and H2′ and missing contacts between H6 and H1′ protons clearly establish an *anti* orientation with glycosidic torsion angles in the 180° range at low temperatures (spectral region not shown). For this conformation, another short intermolecular distance of about 3.3 Å connects imino protons hydrogen-bonded to the 2-carbonyl group and the anomeric H1′ proton (Figure 4).

These considerations allow the straightforward assignment of all imino resonances. From their NOE contacts, A and D can be associated with imino protons hydrogen-bonded to the 4- and 2-carbonyl in the asymmetric O4 – O2 dimer **III**. Correspondingly, B and C arise from the symmetric O4 – O4 and O2 – O2 dimers **I** and **II**, respectively. Additional weak crosspeaks between downfield-shifted imino protons and H1′, as well as between upfield-shifted imino protons and H5, can be attributed to intramolecular contacts involving distances greater 4 Å. The observation of individual NMR resonances also allowed us to quantitatively determine the population of the different dimeric species in solution. Deconvoluting the signals by spectral simulation and accounting for the number of equivalent imino protons within the three dimeric structures results in relative populations at 123 K of 1:1:1.6 for dimers **I**, **II**, and **III**. If we take into account the twofold degeneracy of the latter, the relative populations of homodimers indicate that all base-pair configurations are of similar stability and both carbonyl groups contribute almost equally as proton acceptor sites to the uridine dimers.

We also recorded ^{13}C NMR spectra of **1** in freon to follow the chemical shift of the C2- and C4-carbonyl carbon as a function of temperature (Figure 5). There is a downfield shift

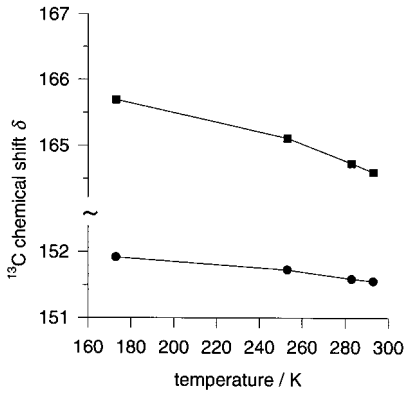

Figure 5. Temperature dependence of the C2 (●) and the C4 (■) ^{13}C chemical shifts of **1** in freon.

for both resonances upon cooling owing to increased self-association. The larger shift of C-4 relative to C-2 in freon is consistent with temperature-dependent measurements on a uridine derivative in acetonitrile,[9c] precluding significant solvent effects on the relative dimer populations. Two factors may account for the ^{13}C NMR data: i) larger perturbations experienced by the C-4 carbonyl carbon in a hydrogen bond and/or ii) a larger temperature dependence of the association constant for O4 – O4 self-associates. The latter implies different enthalpy and entropy changes, ΔH° and ΔS°, for the formation of the O4 – O4 and O2 – O2 homodimers. Given roughly equal populations at 123 K, a growing fraction of

0947-6539/98/0404-0624 $ 17.50+.50/0 *Chem. Eur. J.* **1998**, *4*, No. 4

O2–O2 homodimers would be anticipated with increasing temperature. Clearly, such a situation is not supported by the available experimental data, nor is it compatible with the larger shift of the C-4 relative to the C-2 ^{13}C signal in concentration-dependent NMR measurements at temperatures > 300 K.[9a, c] Consequently, the carbonyl carbons are likely to be differently affected in a hydrogen bond, prohibiting a quantitative analysis of ^{13}C NMR data without knowledge of the individual perturbation in their electron distribution.

*[3-^{15}N]-2′-deoxy-4-thiouridine (**2**):* The temperature dependence of the imino proton resonance for the 4-thio analogue **2** in freon is shown in Figure 6a. Again, a downfield shift of the signal with decreasing temperature is indicative of a self-association process. However, unlike that of **1**, the imino

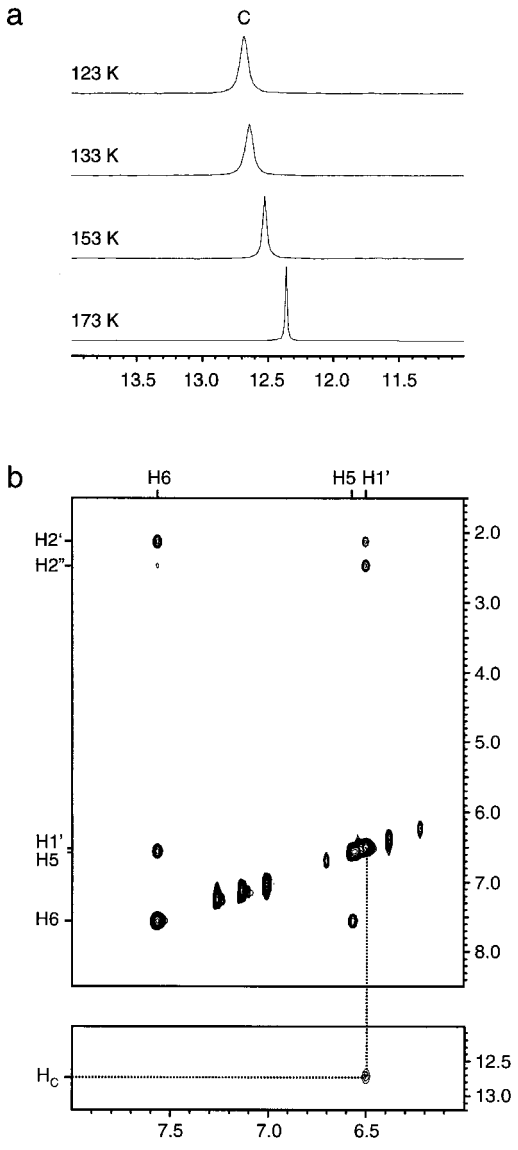

Figure 6. a) Imino proton spectral region of $^1H\{^{15}N\}$ NMR spectra of **2** in freon as a function of temperature. b) Portion of a $^1H\{^{15}N\}$ 2D NOE spectrum of **2** in freon showing regions with imino–base/H1′ (bottom) and base/H1′–base/sugar proton crosspeaks (top). The connectivity between the imino and H1′ proton is indicated by the dotted line. The spectrum was acquired at 123 K with a 100 ms mixing time.

resonance of **2** undergoes no exchange broadening and there is only a continuously increasing linewidth with decreasing temperature owing to a slower molecular reorientation. At 123 K the chemical shift of the imino proton has reached its limiting value and does not change when the temperature is further decreased. If we disregard the possibility of complete signal overlap, the observation of a single resonance at low temperatures indicates the existence of only one dimer in solution.

To further characterize the self-association mode of **2**, we performed a 2D NOE experiment at 123 K. Portions of the spectrum are shown in Figure 6b. Of course, the above-mentioned considerations for **1** concerning interproton distances are also valid in this case. Crosspeaks between H1′ and H2′/H2″ protons, a strong crosspeak between H5 and H6 and the absence of any contacts between H5 and sugar protons clearly identify the partially overlapping H1′ and H5 resonances. Moreover, a strong crosspeak between H6 and H2′ and the absence of a NOE connectivity between H6 and H1′ indicates an *anti* glycosidic torsion angle for **2**. For the imino proton a prominent crosspeak to the H1′ proton is observed, that is, the NH proton can be assigned to H_C of the O2–O2 dimer **II**. As there is no indication of an imino–H5 contact, the presence of significant amounts of dimeric structures **I** and **III**, which use the 4-thiocarbonyl as proton acceptor, can be safely precluded. The sulfur atom is known to be inferior to the oxygen as a proton acceptor and obviously cannot effectively compete as acceptor in a dimer. Assuming a similar situation at higher temperatures, the fourfold decrease in the association constant for **2** at 293 K can be attributed to the statistical disadvantage of having only one efficient H-bond acceptor site, whereas for **1** all four base-pair arrangements are nearly isoenergetic and contribute equally to the dimer (see Table 1).

*[3-^{15}N]-6-oxadihydrouridine (**3**):* For the uridine analogue **3**, a shift in the equilibrium towards a dimeric structure at lower temperatures results in a downfield shift of the imino proton signal, as was observed for **1** and **2** (Figure 7a). At 143 K the resonance is noticeably broadened but sharpens again at 123 K. At the same temperature, a second signal of much lower intensity appears at $\delta = 10.63$, upfield of the larger resonance at $\delta = 10.80$. Deconvolution by peak fitting gives an integral ratio of 8 to 1. The large population differences associated with these two signals can account for the relatively small exchange broadening around the coalescence point at 143 K when compared to **1**.

Portions of the 2D NOE spectrum of **3** acquired at 118 K are shown in Figure 7b. Apparently the higher molecular weight and hence the slower molecular reorientation increases the linewidth of individual resonances of **3** compared with **1** and **2.** Nevertheless, by means of additional $^1H-^{13}C$ correlation data (not shown) all resonances have been unambiguously assigned. Connectivity patterns expected between base and sugar protons for **3** are similar to those of **1,** except for the absence of H6 protons in the 6-oxa analogue. This prevents a distinction between *syn* and *anti* conformations based on H6-H1′/H2′ contacts. However, the observation of a NOE crosspeak between the imino signal at $\delta = 10.80$ and H1′ not only identifies dimer **II** with O2–O2 geometry as the predominant

structure at this temperature, but also precludes a *syn* conformation with corresponding distances to H1′ > 4.5 Å. Having assigned the downfield signal to the O2 – O2 configuration, we must attribute the upfield-shifted low-intensity NH signal to imino protons hydrogen-bonded to the 4-carbonyl in an O4 – O4 and/or O4 – O2 geometry. On the basis of energy-minimized models, intermolecular distances between imino protons hydrogen-bonded to O4 and the two H5 protons in **3** are in the range 3.6 – 3.9 Å and should give rise to observable NOE contacts. However, the low intensity of the

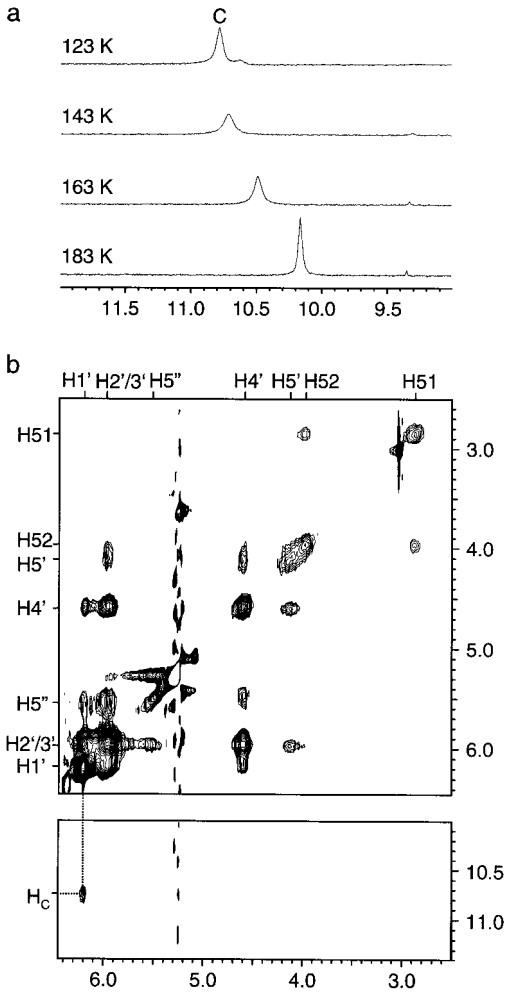

Figure 7. a) Imino proton spectral region of $^1H\{^{15}N\}$ NMR spectra of **3** in freon as a function of temperature. b) Portion of a $^1H\{^{15}N\}$ 2D NOE spectrum of **3** in freon showing imino – base/sugar (bottom) and base/sugar – base/sugar proton crosspeaks (top). The connectivity between the imino and H1′ proton is indicated by the dotted line. The spectrum was acquired at 118 K with a 60 ms mixing time.

upfield-shifted imino resonance does not permit the detection of any crosspeak to H5 protons. Despite the strong preference of the 6-oxa analogue to associate in an O2 – O2 geometry, the population of complexes formed through the C-4 carbonyl group is more than 10 % of the total; this fact may account for the somewhat larger association constant determined for **3** compared with that of **2** in a chloroform solution.

Hydrogen bond strength: ^1H NMR chemical shifts of H-bonded protons are often used as indicators of the hydrogen bond energy. Thus, observation of a highly deshielded proton suggests its participation in a strong hydrogen bond. Based on a simple electrostatic model, the hydrogen bond energy should increase as the donor becomes more acidic and the acceptor becomes more basic as a result of an increase in partial positive and partial negative charge on the donor and acceptor, respectively.[18] In order to obtain partial charges on the two H-bond acceptor sites, we performed 6-31 G* ab initio calculations on the 1-methyl derivatives of **1**, **2**, and **3**. Atomic charges on the carbonyl oxygen or sulfur derived from fits to electrostatic potentials are shown for all three bases in Figure 8. Although these values were determined for the gas

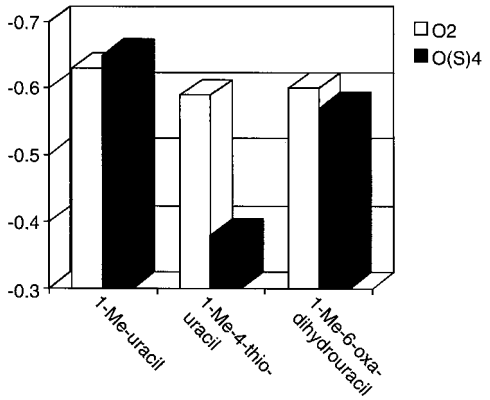

Figure 8. Electrostatic fit charges on the O2 and O(S)4 atom for the 1-methyl derivatives of **1**, **2**, and **3**, obtained from 6-31 G* ab initio calculations.

phase, there is nevertheless a qualitative agreement between calculated charges and experimental ^1H chemical shifts. In the case of uridine, the calculated difference in partial charges on the O-4 and O-2 atom is small, but in line with a more downfield-shifted imino proton H-bonded to the 4-carbonyl. In contrast, for the 6-oxa- and in particular for the 4-thio analogue a higher negative charge resides on the O-2 oxygen, indicating a stronger hydrogen bond through the 2-carbonyl group. However, from the small ^1H chemical shift differences of A/B or C/D imino protons in the uridine dimer it becomes apparent that geometrical factors may contribute to the hydrogen bond energy as well (see Figure 3). It should also be emphasized that it is not only the H-bond energy which determines the dimer population. Rather, the dimer free energy is also influenced by solvation effects and by additional long-range and steric interactions.

^{15}N NMR spectroscopy: The ^{15}N isotope was found to be a sensitive probe for hydrogen bonding in nucleosides[9d, 19] and DNA fragments.[20a–c] To explore the potential of ^{15}N chemical shifts in monitoring the formation and strength of hydrogen bonds in more detail, we acquired temperature-dependent ^{15}N NMR spectra of the specifically 3-^{15}N-labeled nucleosides **1**, **2**, and **3** in freon. For all three nucleobases self-association results in similar chemical shift changes for the imino proton and the imino nitrogen, yet in all cases changes in ^{15}N chemical shifts are slightly smaller than changes in the ^1H

0947-6539/98/0404-0626 $ 17.50+.50/0 *Chem. Eur. J.* **1998**, *4*, No. 4

chemical shift. Thus, lowering the temperature from 293 K to 173 K leads to a downfield shift of the NH proton and nitrogen resonances of **1** by 2.14 and 1.90 ppm, respectively (data not shown). We found no change in the $^{1}H-^{15}N$ ^{1}J scalar coupling upon hydrogen bond formation, in contrast to previous studies on A–U base pairs.[19]

Because proton chemical shifts are also indicative of the hydrogen bond strength, we wanted to examine possible correlations between ^{1}H and ^{15}N chemical shifts for the various hydrogen-bonded self-associates. For this purpose we acquired 2D $^{1}H-^{15}N$ heteronuclear multiple-quantum coherence (HMQC) spectra at temperatures low enough for observation of the individual dimers. A representative $^{1}H-^{15}N$ HMQC spectrum of **1** at 123 K is shown in Figure 9.

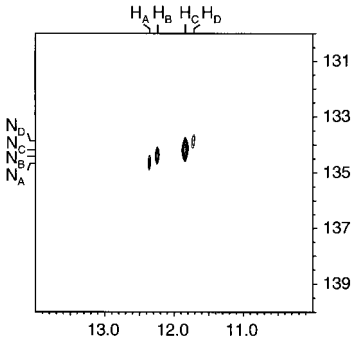

Figure 9. Portion of a gradient-selected $^{1}H-^{15}N$ HMQC spectrum of **1** in freon at 123 K.

Obviously, ^{1}H and ^{15}N chemical shifts correlate among the dimeric species of nucleoside **1**, in that NH groups with a more downfield-shifted proton resonance also have a more downfield-shifted ^{15}N resonance. However, this correlation is not necessarily valid among different nucleosides (Table 2). Thus,

Table 2. ^{1}H and ^{15}N chemical shifts of the NH imino group of dimeric nucleosides **1**, **2**, and **3** at 123 K in freon.

Nucleoside	Dimer	δ (^{1}H)	δ (^{15}N)
1	O2–O4	12.36	134.64
	O4–O4	12.24	134.36
	O2–O2	11.84	134.17
	O2–O4	11.72	133.84
2	O2–O2	12.69	133.32
3	O2–O2	10.80	125.22
	O2(4)–O4	10.63	–[a]

[a] Not observed.

in contrast to its 3-^{15}N signal, the imino proton resonance of dimeric **2** is most downfield-shifted among all dimers of **1**, **2**, and **3**. For dimeric **3**, both ^{1}H and ^{15}N resonances are most upfield-shifted, but no crosspeak could be observed for the low-intensity ^{1}H resonance in a HMQC spectrum at 123 K for reasons of sensitivity (see Figure 7a). Clearly, ^{15}N NMR spectroscopy will be particularly useful under conditions of fast imino proton exchange in protic solvents or in the case of oligonucleotides where proton resonances severely overlap.

Conclusions

The results obtained from low-temperature NMR measurements show that all possible cyclic uridine homodimers are of equal stability and coexist in solution. However, chemical shifts of the H-bonded proton and nitrogen indicate that hydrogen bonds through the 4-carbonyl are more stable than hydrogen bonds through the 2-carbonyl; this fact is consistent with ab initio calculations.

The introduction of modifications, as in the 6-oxa and 4-thio analogue, significantly reduces the probability of the 4-carbonyl participating in hydrogen bonding, and only O2–O2 dimers are observed for the 4-thio analogue at low temperatures. Obviously, this situation results in a statistical disadvantage of dimer formation for the two analogues and might explain the lower association constants compared with uridine, with its four nearly isoenergetic configurations. However, care must be exercised when interpreting association constants at 293 K because we only know relative populations at low temperatures. While enthalpies ΔH° for the formation of the uridine homodimers are unlikely to be very different, this need not be true for the two uridine analogues resulting in changing populations at higher temperatures.

Modified pairing geometries may have important implications in view of the post-transcriptional introduction of the 4-thio group into uridine. However, knowledge of the favored H-bond donor and acceptor sites of various natural and nonnatural nucleosides is not only important for understanding nucleic acid structures, which are mostly determined by base–base hydrogen bonding. It is also a prerequisite for the rational design of new base analogues for a wide range of biochemical and pharmaceutical applications. Moreover, the results presented also provide thermodynamic and structural data against which theoretical calculations can be tested.

Experimental Section

General: NMR experiments were performed on a Bruker AMX500 spectrometer. Temperatures were adjusted by a Eurotherm variable temperature unit to an accuracy of $\pm 1.0\,^{\circ}C$. ^{1}H and ^{13}C chemical shifts in chloroform at 293 K were referenced relative to $CHCl_3$ ($\delta_H = 7.24$, $\delta_C = 77$) and in a freon mixture relative to $CHClF_2$ ($\delta_H = 7.13$, $\delta_C = 116.36$). For ^{15}N chemical shifts an external reference of $^{15}NH_4Cl$ in 10% HCl was used ($\delta_N = 0$). Signal integrals were determined with a Lorentzian curve-fitting routine of the UXNMR software package. Concentration-dependent chemical shifts were fitted with an appropriate equation by employing the Marquardt–Levenberg algorithm. Electrostatic potentials were calculated with SPARTAN, Version 4.1.1.

Materials: The deuterated freon mixture $CDClF_2/CDF_3$ was prepared as described[16b] and handled on a vacuum line, which was also used for the sample preparation.$^{15}NH_4Cl$ was purchased either from Chemotrade, Leipzig (label 95%) or Deutero GmbH, Kastellaun (label 99%). All reactions were followed by TLC on silica gel plates (Merck silica gel 60 F_{254}). If necessary, solvents were dried by standard procedures prior to use.

[3-^{15}N]-3′,5′-Diacetyl-2′-deoxyuridine (1): Published methods described for ribonucleosides were adapted for the synthesis of **1**.[21] After acetylation of 2′-deoxyuridine with acetic anhydride in dry pyridine, the 3′,5′-diacetyl-2′-deoxyuridine was *N*-nitrated with trifluoroacetic anhydride and NH_4NO_3 in cold anhydrous CH_2Cl_2. Treatment of the resulting 3′,5′-diacetyl-2′-deoxy-3-nitrouridine with $^{15}NH_3$ for 5 days at room temperature and final

purification by HPLC (SiO_2) with AcOEt as eluent afforded pure **1**. Overall yield: 31 %. ^{1}H NMR (500 MHz, 293 K, $CDCl_3$): $\delta = 2.08$, 2.09 (2 s, 6 H; $2CH_3$), 2.14 (m, 1 H; H2′), 2.51 (m, 1 H; H2″), 4.24 – 4.35 (m, 3 H; H4′, H5′, H5″), 5.18 (m, 1 H; H3′), 5.77 (d, ^3J(H,H) = 8.2 Hz, 1 H; H5), 6.26 (dd, 1 H; H1′), 7.47 (d, ^3J(H,H) = 8.2 Hz, 1 H; H6), 9.43 (d, ^1J(N,H) = 91 Hz, 1 H; H3); ^{13}C NMR (125 MHz, 293 K, $CDCl_3$): $\delta = 20.82$, 20.90 ($2CH_3$), 37.81 (C2′), 63.81 (C5′), 74.05 (C3′), 82.30 (C4′), 85.23 (C1′), 102.96 (d, ^2J(N,C) = 7 Hz; C5), 138.80 (C6), 150.17 (d, ^1J(N,C) = 18 Hz; C2), 163.05 (d, ^1J(N,C) = 10 Hz; C4), 170.25, 170.44 ($2CH_3CO$).

[3-^{15}N]-3′,5′-Diacetyl-2′-deoxy-4-thiouridine (**2**): [3-^{15}N]-3′,5′-diacetyl-2′-deoxy-4-thiouridine was prepared from **1** (940 mg, 3 mmol) in analogy to published procedures for the benzoyl derivative.[22] After purification 690 mg of **2** were obtained. Yield: 71 %. ^{1}H NMR (500 MHz, 293 K, $CDCl_3$): $\delta = 2.08$, 2.09 (2 s, 6 H; $2CH_3$), 2.14 (m, 1 H; H2′), 2.56 (m, 1 H; H2″), 4.28 – 4.36 (m, 3 H; H4′, H5′, H5″), 5.19 (m, 1 H; H3′), 6.19 (dd, 1 H; H1′), 6.42 (d, ^3J(H,H) = 7.6 Hz, 1 H; H5), 7.33 (d, ^3J(H,H) = 7.6 Hz, 1 H; H6), 9.40 (d, ^1J(N,H) = 94 Hz, 1 H; H3); ^{13}C NMR (125 MHz, 293 K, $CDCl_3$): $\delta = 20.80$, 20.88 ($2CH_3$), 38.02 (C2′), 63.69 (C5′), 73.96 (C3′), 82.67 (C4′), 85.85 (C1′), 113.62 (C5), 133.27 (C6), 147.39 (d, ^1J(N,C) = 18 Hz; C2), 170.18, 170.39 ($2CH_3CO$), 189.47 (d, ^1J(N,C) = 8 Hz; C4).

[3-^{15}N]-2′,3′,5′-Tribenzoyl-6-oxadihydrouridine (**3**): [3-^{15}N]-6-oxadihydrouracil was synthesized with minor modifications according to literature procedures.[23, 24] Starting with $^{15}NH_3$, the free heterocyclic base was obtained in three steps. The nucleoside was subsequently synthesized by the Vorbrüggen method of glycosylation.[25] Accordingly, [3-^{15}N]-6-oxadihydrouracil (250 mg, 2.16 mmol) and 1-*O*-acetyl-2,3,5-tri-*O*-benzoyl-β-D-ribofuranose (1.09 g, 2.16 mmol) were dissolved in dry acetonitrile (32 mL). Trimethylchlorosilane (0.36 mL) and hexamethyldisilazane (0.22 mL) were added and, after addition of $SnCl_4$ (0.3 mL) in dry acetonitrile (10 mL), the reaction mixture was stirred at room temperature for 3 h. Recrystallization from ethanol and HPLC purification (SiO_2, hexane/AcOEt 75:25) afforded pure **3**. Yield: 73 %. ^{1}H NMR (500 MHz, 293 K, $CDCl_3$): $\delta = 4.18$ (d, ^2J(H,H) = 15.6 Hz, 1 H; H5A), 4.45 (d, ^2J(H,H) = 15.6 Hz, 1 H; H5B), 4.46 (dd, ^2J(H,H) = 12.5 Hz, ^3J(H,H) = 3.7 Hz, 1 H; H5″), 4.65 (m, 1 H; H4′), 4.85 (dd, ^2J(H,H) = 12.5 Hz, ^3J(H,H) = 3.7 Hz, 1 H; H5′), 5.85 (t, ^3J(H,H) = 5.0 Hz, 1 H; H3′), 6.12 (t, ^3J(H,H) = 5.3 Hz, 1 H; H2′), 6.17 (d, ^3J(H,H) = 5.6 Hz; H1′), 7.32 – 8.10 (m, 15 H; ArH), 8.91 (d, ^1J(N,H) = 92 Hz, 1 H; H3); ^{13}C NMR (125 MHz, 293 K, $CDCl_3$): $\delta = 63.4$ (C5′), 70.5 (C2′), 70.6 (C5), 71.8 (C3′), 80.0 (C4′), 87.2 (C1′).

Acknowledgments: This work was supported by the Deutsche Forschungsgemeinschaft (Bonn – Bad Godesberg), and the Fonds der Chemischen Industrie (Frankfurt). We thank Dr. N. S. Golubev, Institute of Antibiotics and Enzymes, St. Petersburg, for introducing us to the low-temperature NMR technique, and R. Zander for his assistance with the chemical syntheses.

Received: October 13, 1997 [F852]

[1] J. H. van de Sande, N. B. Ramsing, M. W. Germann, W. Elhorst, B. W. Kalisch, E. v. Kitzing, R. T. Pon, R. C. Clegg, T. M. Jovin, *Science* **1988**, *241*, 551 – 557.

[2] N. T. Thuong, C. Hélène, *Angew. Chem.* **1993**, *105*, 697 – 723; *Angew. Chem. Int. Ed. Engl.* **1993**, *32*, 666 – 690.

[3] a) T. R. Cech, S. H. Damberger, R. R. Gutell, *Nat. Struct. Biol.* **1994**, *1*, 273 – 280; b) M. Grüne, J. P. Fürste, S. Klussmann, V. A. Erdmann, L. R. Brown, *Nucleic Acids Res.* **1996**, *24*, 2592 – 2596; c) S. E. Lietzke, C. L. Barnes, J. A. Berglund, C. E. Kundrot, *Structure* **1996**, *4*, 917 – 930.

[4] A. D. Hamilton, D. J. van Engen, *J. Am. Chem. Soc.* **1987**, *109*, 5035 – 5036.

[5] C. Hélène, J.-J. Toulmé, *Biochim. Biophys. Acta* **1990**, *1049*, 99 – 125.

[6] a) A. Pohorille, S. K. Burt, R. D. MacElroy, *J. Am. Chem. Soc.* **1984**, *106*, 402 – 409; b) J. Pranata, S. G. Wierschke, W. L. Jorgensen, *ibid.* **1991**, *113*, 2810 – 2819; c) K. I. Trollope, I. R. Gould, I. H. Hillier, *Chem. Phys. Lett.* **1993**, *209*, 113 – 116; d) I. R. Gould, P. A. Kollman, *J. Am. Chem. Soc.* **1994**, *116*, 2493 – 2499.

[7] a) L. Katz, S. Penman, *J. Mol. Biol.* **1966**, *15*, 220 – 231; b) R. A. Newmark, C. R. Cantor, *J. Am. Chem. Soc.* **1968**, *90*, 5010 – 5017; c) L. D. Williams, B. Chawla, B. R. Shaw, *Biopolymers* **1987**, *26*, 591 – 603; d) Y. Kyogoku, R. C. Lord, A. Rich, *Proc. Natl. Acad. Sci. USA* **1967**, *57*, 250 – 257; e) G. Lancelot, C. Hélène, *Nucleic Acids Res.* **1979**, *6*, 1063-1072; f) J. Sartorius, H.-J. Schneider, *Chem. Eur. J.* **1996**, *2*, 1446 – 1452.

[8] Y. Kyogoku, R. C. Lord, A. Rich, *J. Am. Chem. Soc.* **1967**, *89*, 496 – 504.

[9] a) H. Iwahashi, Y. Kyogoku, *J. Am. Chem. Soc.* **1977**, *99*, 7761 – 7765; b) M. I. Burgar, D. Dhawan, D. Fiat, *Org. Magn. Reson.* **1982**, *20*, 184 – 190; c) H. M. Schwartz, M. MacCoss, S. S. Danyluk, *J. Am. Chem. Soc.* **1983**, *105*, 5901 – 5911; d) P. Strazewski, *Helv. Chim. Acta* **1995**, *78*, 1112 – 1143.

[10] K. Weisz, J. Jähnchen, H.-H. Limbach, *J. Am. Chem. Soc.* **1997**, *119*, 6436 – 6437.

[11] R. Masingale, S. R. Bryant, C. G. Skinner, J. Nash, P. F. Kruse, Jr., *J. Med. Chem.* **1969**, *12*, 152.

[12] Note that a nonconventional numbering of the oxadiazine ring system in **3** was adopted to emphasize the analogy to the uracil base.

[13] W. Saenger, *Principles of Nucleic Acid Structure*, Springer, Heidelberg, **1984**, and references therein.

[14] P. T. Berkowitz, R. K. Robins, P. Dea, R. A. Long, *J. Org. Chem.* **1976**, *41*, 3128 – 3132.

[15] D. W. Green, F. S. Mathews, A. Rich, *J. Biol. Chem.* **1962**, *237*, 3573 – 3575.

[16] a) S. N. Smirnov, N. S. Golubev, G. S. Denisov, H. Benedict, P. Schah-Mohammedi, H.-H. Limbach, *J. Am. Chem. Soc.* **1996**, *118*, 4094 – 4101; b) N. S. Golubev, S. N. Smirnov, V. A. Gindin, G. S. Denisov, H. Benedict, H.-H. Limbach, *ibid.* **1994**, *116*, 12055 – 12056; c) N. S. Golubev, G. S. Denisov, S. N. Smirnov, D. N. Shchepkin, H.-H. Limbach, *Z. Phys. Chem.* **1996**, *196*, 73 – 84.

[17] K. Wüthrich, *NMR of Proteins and Nucleic Acids*, Wiley Intersciene, New York, **1986**, pp. 205 – 214.

[18] S.-O. Shan, S. Loh, D. Herschlag, *Science* **1996**, *272*, 97 – 101.

[19] C. D. Poulter, C. L. Livingston, *Tetrahedron Lett.* **1979**, *9*, 755 – 758.

[20] a) X. Gao, R. A. Jones, *J. Am. Chem. Soc.* **1987**, *109*, 3169 – 3171; b) B. Goswami, B. L. Gaffney, R. A. Jones, *ibid.* **1993**, *115*, 3832 – 3833; c) Y. Rhee, C. Wang, B. L. Gaffney, R. A. Jones, *ibid.* **1993**, *115*, 8742 – 8746.

[21] X. Ariza, V. Bou, J. Vilarrasa, *J. Am. Chem. Soc.* **1995**, *117*, 3665 – 3673.

[22] G. Kupferschmitt, J. Schmidt, Th. Schmidt, B. Fera, F. Buck, H. Rüterjans, *Nucleic Acids Res.* **1987**, *15*, 6225 – 6241.

[23] R. Deghenghi, *Org. Synth. Coll. Vol. 5* **1973**, 645 – 646.

[24] C. Bennouna, F. Petrus, J. Verducci, *J. Heterocycl. Chem.* **1979**, *16*, 161 – 167.

[25] H. Vorbrüggen, B. Bennua, *Chem. Ber.* **1981**, *114*, 1279 – 1286.

  0947-6539/98/0404-0628 $ 17.50+.50/0